

26 **Abstract**

27 The accurate estimation of plant transpiration is critical to the fields of hydrology, plant
28 physiology, and ecology. Among the various methods of measuring transpiration in the field, the
29 sap flow methods based on heat pulses offers a cost-effective and energy efficient option to
30 directly measure the plant-level movement of water through the hydraulically active tissue.
31 While authors have identified several possible sources of error in these measurements, one of the
32 most common sources is misalignment of the sap flow probes due to user error. Though the
33 effects of probe misalignment are well documented, no device or technique has been universally
34 adopted to ensure the proper installation of sap flow probes. In this paper we compare the
35 magnitude of misalignment errors among a 5 mm thick drilling template, a 10 mm thick drilling
36 template, and a custom designed, field-portable drill press. The different techniques were
37 evaluated in the laboratory using a 7.5 cm wood block and in the field, comparing differences in
38 measured sap flow. Based on analysis of holes drilled in the wood block, we found that the
39 portable drill press was most effective in assuring that drill holes remained parallel, even at 7.5
40 cm depth. In field installations, nearly 50% of holes drilled with a 5 mm template needed to be
41 redrilled while none needed to be when drilled with the drill press. Widespread use of a portable
42 drill press when implementing the heat pulse method would minimize alignment uncertainty and
43 allow a clearer understanding of other sources of uncertainty due to variability in tree species,
44 age, or external drivers or transpiration.

45

46

47

48

49 **Introduction**

50 Accurate estimation of plant transpiration is of vital importance to the hydrologic,
51 agricultural, ecological, and climate sciences. Transpiration can represent between 60-80% of the
52 water returned to the atmosphere, depending on the ecosystem (Jasechko et al., 2013). While
53 there are a variety of techniques used to quantify transpiration or partition total
54 evapotranspiration, sap flow measurements are one of the most cost-effective options for
55 measuring tree-level fluxes. The different sap flow methods fall broadly into two categories, 1)
56 heat dissipation, including thermal dissipation (TD; Granier, 1985) and transient thermal
57 dissipation (TTD; Do & Rocheteau, 2002) and 2) heat-pulse sap-flux methods, including the
58 compensation heat pulse (CHP; Swanson & Whitfield, 1981), T_{max} (Cohen et al., 1981), heat
59 ratio (HR; Burgess et al., 2001), and dual method approach (Forster, 2019).

60 Of these, the TD method continues to be the most widely implemented due to its general
61 ease of use and accessibility, despite noted systematic biases (Flo et al., 2019). While not
62 sensitive to sensor installation, the empirical equation used to derive sap flux density has been
63 identified as a source of uncertainty. Originally considered to be universal across all wood types,
64 the calibration parameters of the TD method have been shown to be species specific and require
65 rigorous calibration to obtain accurate results (Bush et al., 2010; Fuchs et al., 2017; Steppe et al.,
66 2010). This uncertainty, species-specific calibration, and a general underestimation of sap flow,
67 has led some researchers to recommend the heat-pulse methods, particularly when absolute flow
68 estimations are required (Flo et al., 2019; Vandegehuchte & Steppe, 2013).

69 Unlike the TD method, there is little fundamental uncertainty by species via the family of
70 heat pulse (HP) methods as long as thermal diffusivity and physiological parameters, such as
71 moisture content and sap wood density, are known (Flo et al., 2019; Vandegehuchte & Steppe,

72 2012). However, the most common source of uncertainty may be caused by error in probe
73 placement (Cohen et al., 1981; Forster, 2017; Figure 1) given that HP methods typically require
74 the drilling of three near-perfectly aligned and spaced holes for probes. While probe
75 misalignment can be minimized by implementing a proper drill guide, use of these tools is not
76 ubiquitous, or their use is not always detailed in the methods section.

77 Probe placement error can be characterized in three ways (Figure 1): vertical
78 misalignment, lateral misalignment, and angular misalignment. Vertical and lateral
79 misalignments are characterized by any offset along the y or x axis, respectively, at the outer
80 surface of the tree. While most common when drilling “free hand”, these misalignments can
81 occur due to improperly constructed or worn drill guides, though they can be easily detected in
82 the field with a ruler or level. Angular misalignment is characterized by an installation in which
83 the drill hole does not remain perpendicular to the tree surface as it is drilled into the tree. This
84 misalignment can be more difficult to detect, and can be caused by user error (i.e., drill was not
85 held level during installation) or narrow drill guides which allow the bit to deviate in the
86 sapwood.

87 There has been relatively little work to quantify error in sap flow measurements due to
88 misalignment when compared to the frequent use of the sap flow methods. In a laboratory
89 experiment using a container filled with glass beads attached to a peristaltic pump, angular
90 misalignment of 4° resulted in errors as high as 8%, 13%, 45% for the HR, Tmax, and CHP
91 methods, respectively (Ren et al., 2017). While Ren et al. (2017) proposed corrections for
92 angular misalignment for the common heat pulse methods, it was noted that these corrections
93 resulted in systematic underestimation of sap flow. In a greenhouse experiment conducted in
94 potted *Eucalyptus marginata* situated on weighing lysimeters, Bleby et al. (2004) found vertical

95 misalignment of only 2 mm resulted in a 100% error in sap velocity estimates, the largest source
96 of error identified in a comprehensive review of biases. However, *in situ* calibrations have been
97 developed to rectify this type of misalignment (Liu et al., 2013) as long as the vertical
98 misalignment is within a suitable threshold.

99 Despite this limited work on quantifying the effects of misalignment error, there has been
100 widespread recognition of the need to develop techniques to identify, minimize, or rectify
101 misalignment errors. The over-length method inserts long blank probes into freshly drilled holes
102 to try to detect the presence of angular misalignment; probe spacings could then be recalculated
103 using trigonometry (Dye et al., 1991; Hatton et al., 1995). Inverse mathematical methods have
104 been applied to use measured heat pulses to calculate the distance between probes when sap flux
105 is zero (such as during rainy nighttime conditions) and thermal diffusivity is known. Previously
106 assumed distances are replaced with new calculated value as an *in situ* correction (Burgess et al.,
107 2001; Forster, 2019). The saturation method, an assessment of predicted sap flow at assumed
108 zero flow conditions, has been used to shift, or offset the error due to misalignment, of entire
109 time series of data as long as the raw heat pulse velocity is within a suitable threshold, typically
110 -5 to 5 cm hr^{-1} (Hogg & Hurdle, 1997; *Implexx Manuals and Guides* | *Implexx Sense*, 2019;
111 Looker et al., 2016; M. Zeppel et al., 2010). Using the same technique as the saturation method,
112 the cut stem method artificially induced zero flow conditions by severing the sap stream (Roddy
113 & Dawson, 2013). While this method has been considered more accurate than the saturation
114 method, it required destructive harvesting of the plant.

115 The most common technique to properly align sap flux probes has been to use a drilling
116 template or guide (Forster, 2017; Ren et al., 2017; Vandegehuchte & Steppe, 2013).

117 In the few cases where published literature describes templates, they are typically constructed of
118 steel and no more than 10 mm in depth (Bleby et al., 2004; Burgess et al., 2001), although
119 templates as thick as 20 mm have been used (Dye et al., 1991; McJannet & Fitch, 2004). While
120 these guides can be useful in minimizing lateral and vertical misalignment, they can be less
121 effective in minimizing angular misalignment. Because there are minimal options currently
122 available to prevent angular misalignment, we developed a portable drill press operated by a
123 handheld cordless drill designed to accurately align probes of all lengths in mature trees.

124 This drill press was designed with the intention of improving errors due to misalignment,
125 as well as ease of use. This device needed to be relatively light weight and allow the drill bit to
126 move up and down independent of the frame secured to the tree. The initial prototype included a
127 prefabricated portable drill guide (portable drill guide #4525, Rockler), however the tolerance on
128 the bearings and drill carriage proved insufficient for accurate drilling. We therefore opted to
129 craft a custom-built drill carriage on precision linear bearings and rods attached directly to a
130 movable mount on the frame of the press.

131 Despite a broad recognition of the need to avoid misalignment, there has been no
132 systematic assessment of the ability of different templates and guides to minimize alignment
133 error. In this paper, we consider differences in hole alignment error when using guides of
134 different design. This includes templates of different thickness as well as the custom-designed,
135 portable drill press that can be mounted to a tree. Included are details of the design and
136 fabrication of the custom drill press. A standardization of methods for aligning and installing
137 probes for the heat pulse method can enhance repeatability and reduce experimental uncertainty
138 in heat pulse measurements, better allowing the identification of true controls on sap flow such
139 as tree species, tree location, and climate drivers.

140

141 **Methods**

142 An initial section describes the construction of the drill press as well as the templates. Following
143 this is an overview of the two portions of the experimental assessment: 1. comparison of hole
144 alignment when drilled through a wooden block and 2. comparison of sap flow measurements
145 when drilled into actual trees.

146

147 *Drill Press Construction*

148 The drill press was comprised of three main components: 1) the frame, 2) the drill carriage
149 mount, and 3) the drill carriage (Figure 2).

150 The frame of the drill press was constructed of four pieces of lightweight 40-4040C T-
151 slotted aluminum rails. The two lengthwise pieces were cut to 40.64 cm, while the widthwise
152 pieces were cut to 7.62 cm, giving the drill press a total width of 12.7 cm. The rails were
153 connected using 45 series 2 hole- 39mm slotted inside corner brackets. The carriage mount was
154 attached to the frame using two double flanged linear bearings that slid along the lengthwise T-
155 slotted aluminum rails. The inner edges of the two flanged bearings were screwed to a 8.9 x 8.9
156 cm piece of Delrin plastic to ensure unison motion along lengthwise aluminum rails. The 8.9 x
157 8.9 cm Delrin plastic was hollowed out creating a 6.4 x 6.4 cm window for the drill chuck and bit
158 when the carriage was lowered during drilling.

159 The movement of the drill carriage mount was controlled by Velmex UniSlide screw
160 drive model, mounted on the lower widthwise aluminum rail and connected to the 8.9 x 8.9 cm
161 piece of Delrin plastic. The screw drive allowed the drill carriage mount approximately 3 cm of
162 precision motion along the lengthwise slotted aluminum rails. Two 31.75 cm long, 0.95 cm

163 diameter, one-end-threaded linear bearing shafts, each attached to a ¼"-20 tread camera mount
164 located in the center of the flanged bearings, held the drill carriage.

165 The drill carriage was constructed using a 15.2 x 3.2 cm piece of Delrin plastic. On either
166 end of the drill carriage matching the position of the linear bearing shafts, two precision 0.95 cm
167 diameter, 3.8 cm, linear ball bushing bearings were machined into the Delrin plastic. The linear
168 bearings and shaft provide a smooth, controlled in-and-out action for the drill carriage mount. In
169 the center of the drill carriage, four 1.3 cm diameter, 0.79 cm long radial ball bushing bearings
170 were stacked atop each other to create a snug fit to hold the 41BA 1/2-20 Jacobs drill chuck. The
171 drill press was operated using a 20 V handheld cordless drill, and was secured to the trees using
172 ratchet straps (Figure 3). The drill bit was aligned at each probe position by twisting the knob of
173 the Velmex UniSlide screw drive. Beneath the drill carriage, an optional 10 mm drilling template
174 could be aligned with the drill bit and attached to the lengthwise lightweight 40-4040C T-slotted
175 aluminum rails. Installations via the portable drill press were drilled with a 14 cm, No. 54 bit,
176 with approximately 3 cm of the bit inserted into the drill chuck.

177 Both the 5 mm and 10 mm drill templates were constructed out of plate steel, with the
178 guide holes spaced 5 mm apart from each other. A small level guide was attached to the side of
179 each drill template to ascertain vertical alignment. Four holes, one in each corner of the
180 templates, allowed for the ability to secure the template to the tree with short nails or screws.
181 Installations via the templates were drilled with a 11 cm, No. 54 bit, with approximately 3 cm of
182 the bit inserted into the drill chuck.

183 *Method Comparison of Hole Alignment in a Wood Block*

184 Drilling accuracy was compared between the constructed drill press with the optional
185 template (DT), without the optional template (D), a 5 mm deep drilling template (T5), and a 10

186 mm deep drilling template (T10) at both 3.75 cm and 7.5 cm drilling depth. The 3.75 cm depth
187 was selected to represent the standard drilling depth for most commercial sensors (i.e. TDP-30
188 from Dynamax), while the 7.5 cm depth was selected to highlight potential errors in deep
189 sapwood studies such as Ford et al., (2004). Using each drill guide device, six drilling attempts
190 were made in a 7.5 cm block of pine wood. The wood block was strapped to a tree to simulate
191 field conditions while not requiring destructive measures to analyze the positioning of the drilled
192 holes. Following the drilling, the wood block was cut in half along the depth of the block to
193 analyze the positioning of the holes in a standard deployment (3.75 cm), as well as the full 7.5
194 cm depth of the board. The front, middle and back of the wood block was imaged with a
195 mounted and leveled DSLR camera (Nikon D5600). A reference hole was drilled through the
196 depth of the wood block using a machine shop drill press to establish a uniform coordinate
197 system between photos. The x and y coordinates of the holes were measured using ImageJ
198 (Image J, NIH, USA, <http://rsbweb.nih.gov/ij/>).

199 The vertical and lateral alignment of the drill attempts were assessed via the distance
200 from the ideal positioning of -5, 0, and 5 mm for the upstream, heater, and downstream probes,
201 respectively, on the front of the wood block. In order to establish a uniform reference for each
202 drill attempt, the heater probe was assumed to be perfectly aligned (i.e., 0,0 on an x,y coordinate
203 system) in each drill attempt, and only the up- and downstream probes were measured for
204 vertical and lateral misalignment. The mean and standard deviation of the misalignments were
205 measured for each drill guide type (i.e., drill press with the optional drilling template [DT],
206 without [D], 10 mm template [T10], and 5 mm template [T5]).

207 The angular misalignment for each drill attempt was assessed in the vertical and lateral
208 directions. The angle of misalignment was calculated by the arctangent of the depth of the board

209 (i.e., 7.5 cm) and the vertical or lateral distance between the entry and exit wounds. The mean
210 drilling angle, as well as the standard deviation, were assessed to gauge both the precision and
211 accuracy of each drill guide type.

212

213 *Method Comparison of Hole Alignment in Field-Instrument Trees*

214 One *Tsuaga canadensis* (HEM-3) and two *Acer saccharum* (MAP-8 and MAP-13) were
215 instrumented in summer 2022 with a pair of custom sap flux sensors (Beslity et al., 2022), one
216 installed using the custom drill press (D), the second using a drilling template (T5), with the two
217 sensors installed at a 90° angle on the north and east face of the tree. The tree selected for this
218 study were part of a larger ongoing study in Hammond Hill State Forest, Dryden, NY. Each
219 sensor probe was 50 mm in length and contained four independent temperature sensors located at
220 5, 15, 25, and 35 mm. The sensor probes were spaced 5 mm apart from the heater probe in the
221 up- and downstream positions. The sensors collected measurements at 30-minute intervals,
222 skipping the hours of 2100-0100 and 0300-0500 to conserve battery life. All sensors were
223 operational from 6/10/2022 through 7/20/2022.

224 We applied the dual method approach of heat pulse sensing (DMA), a combination of the
225 heat ratio method and Tmax method (Forster, 2019). The standard heat ratio utilizes two sensor
226 probes installed up and downstream of the heater probe. This method was adjusted to calculate
227 differences in the vertical positioning of probes and duration of the applied heat pulse
228 (Kluitenberg et al., 2007):

$$229 \quad V_{h,HRM} = \frac{2D \left(\ln \left(\frac{\Delta T_d}{\Delta T_u} \right) \right)}{x_d + x_u} + \frac{x_d - x_u}{2 \left(t - \left(\frac{t_o}{2} \right) \right)} \quad \text{Eq. 1}$$

230 where $V_{h,HRM}$ is the heat pulse velocity (cm s^{-1}), D is thermal diffusivity ($\text{cm}^2 \text{s}^{-1}$), ΔT_u and ΔT_d
 231 are the changes in temperature upstream and downstream following the heat pulse (K) averaged
 232 between 60 and 100 seconds (Burgess et al., 2001), t_o is the heat pulse duration, and x_d and x_u are
 233 the distances between the heater probe and the down- and upstream sensor probes, respectively.
 234 The thermal diffusivity for each instrumented tree was calculated via the improved methods
 235 detailed by Vandegehuchte & Steppe (2012). Sap wood samples were collected using a 5 mm
 236 increment borer. The sap wood was immediately placed in airtight bags and stored in a cooler
 237 until processed in the laboratory.

238 The Tmax method utilizes a single downstream sensor probe with the equation:

$$239 \quad V_{h,Tmax} = \sqrt{\frac{4D}{t_o} \ln\left(1 - \frac{t_o}{t_m}\right) + \frac{x_d^2}{t_m(t_m - t_o)}} \quad \text{Eq. 2}$$

240
 241 where $V_{h,Tmax}$ is the heat velocity (cm s^{-1}), x is the distance between the heater and downstream
 242 sensor probe, and t_m is the elapsed time (s) for the downstream sensor to reach the maximum
 243 temperature of the heat pulse (Cohen et al., 1981, Kluitenberg & Ham, 2004).

244 The Tmax equation can be rearranged to back-calculate for the distance x between the
 245 probes:

$$246 \quad x = \sqrt{\frac{D4t'_m \ln\left(\frac{t'_m}{t'_m - t_o}\right)(t'_m - t_o)}{t_o}} \quad \text{Eq. 3}$$

247 This does require that D is known and presumes that sap flow velocity is nearly zero, a condition
 248 that is presumed to occur on rainy nights when the vapor pressure deficit is low. This back-
 249 calculation of x allows for non-destructive, in situ comparisons of alignment between the
 250 template and drill press in the field.

251 Additionally, the saturation method (Hogg & Hurdle, 1997) and over-length (Hatton et
252 al., 1995) methods were used to assess suitability of field installations of sensors. In the
253 saturation method, raw heat pulse velocity measurements ($V_{h,HRM}$) measured via the HR method
254 were used to assess the viability of each installment at each thermistor depth by assessing if
255 $V_{h,HRM}$ exceeds a given threshold. Academic literature detailing the saturation method advises
256 using best judgment but rarely gives an explicit threshold for assessing viability. Here, we make
257 use of guidance provided for widely used commercial heat pulse probes from Implexx Sense that
258 indicates a threshold of -5 and 5 cm hr^{-1} (*Implexx Manuals and Guides* | *Implexx Sense*, 2019). If
259 $V_{h,HRM}$ at any depth falls outside this pre-determined threshold during a nighttime precipitation
260 event a reinstallation was considered necessary. In the over-length method, oversized dummy
261 probe were inserted into the drill holes to gauge to lateral alignment of the probes. The distance
262 to the hundredth mm between the probes was measured at the entry (0 mm), middle (25 mm),
263 and end points (50 mm) of the dummy probes using digital calipers (IP54 - 6-Inch Digital
264 Caliper, Baileigh Industrial), and the change in distance between the probes was used to assess
265 the installations. The mean change in distance between the two drill guide types was assessed
266 using a Student's t-test.

267

268 **Results**

269 The drill guides were initially assessed based on lateral, vertical, and angular
270 misalignment in the 7.5 cm thick block. Figure 4 illustrates the position of the exit holes from the
271 wood block for the three different types of drill guides. Qualitatively, it is evident that most exit
272 holes are not perfectly aligned with the entrance holes. However, the actual source of
273 misalignment needs to be determined based on different methods of analyzing hole position.

274 Lateral and vertical alignment were assessed based on absolute position of the holes at
275 entry for the upstream, heater and downstream probes. Suitability of the position of the holes is
276 characterized by the absolute mean and standard deviation. The mean represents aggregate error,
277 while the standard deviation represents the scatter about mean misalignment. While there was no
278 statistical difference between drilling guides (Table 1) in terms of absolute vertical and lateral
279 misalignment as based on standard deviation, T10 did provide a slightly more precise placement
280 of holes than the drill press and T5 in the vertical plane, due to the fixed position of the guide
281 holes in the templates. The need to use the UniSlide screw drive in the drill rig to move the bit to
282 the proper position increased the standard deviation of the hole alignment along the vertical axis
283 (Table 1). When a 10 mm drilling template was attached to the portable drill press, the absolute
284 mean misalignment and standard deviation were further reduced.

285 Angular misalignment was assessed by considering the angle between the actual entry
286 hole (not the ideal entry hole) and the corresponding exit hole. The drill press with and without
287 the attached template outperformed both T10 and T5 when assessing the angle of misalignment
288 (Table 2). The main measure of interest for assessing angular misalignment is the standard
289 deviation of the angle; mean angle represents systematic error but standard deviation represents
290 the reliability of the drill guide type to install parallel, if equally misaligned, holes. In both the
291 vertical and lateral direction, the standard deviation was smallest via the drill press with the
292 attached template, 0.46° and 0.24° , respectively, which represented a more consistent alignment
293 of probes and ensuring the measurement points along the temperature sensors would be more
294 equally spaced across different radial depths. The mean angle of misalignment for the drill press
295 was 0.37° and -0.49° in the vertical and lateral directions, respectively, compared to 1.07° and
296 0.21° for the drill press alone, and -0.36° and -0.93° for T10.

297 In the field, the alignment of drilled holes was estimated using heat pulse data in
298 conjunction with Eqn. 3, as well as the over-length method. Using time differences in heat pulse
299 arrival at different thermistors, Eqn. 3 estimates the distance between the heating probe and
300 sensing probes. Based on this method, the drill press resulted in more parallel holes compared to
301 T5 as measured by the difference in the mean distance between drilled holes (p -value = 0.06),
302 consistent with the experiments made using the wood block. Measured via the inverse
303 mathematical method, the mean absolute change in vertical position from the 5 mm thermistor to
304 the 35 mm thermistor was 0.5 mm for the drill press but over 1.0 mm for the 5 mm template
305 (Figure 5). Using the overlength method, the mean absolute change across the entire length of
306 the probe (50 mm) was 1.5 mm for the drill press and 3.3 mm for the 5 mm template (Figure 5).
307 As with the inverse mathematical method, the drill press resulted in more parallel holed
308 compared to T5 when compared with the overlength method (p -value = 0.11).

309 When comparing the field data between D and T5, the drill press consistently delivered
310 measurements within the acceptable range based on guidance given for the saturation method
311 (Hogg & Hurdle, 1997; *Implexx Manuals and Guides* | *Implexx Sense*, 2019). Across all four
312 depths of the three field-instrumented trees installed via the drill press, the raw heat pulse
313 velocity ($V_{h,HRM}$) measured during a night time precipitation event via the drill press fell within
314 the 5 and 5 cm hr^{-1} threshold, representing a successful installation. Measurements from probes
315 installed via T5 failed to fall within the threshold at 5 of the 12 of the tree-depth combinations.
316 Measurements via T5 at 25 and 35 mm in Hem-3 were unable to be resolved using Eq. 1 due to
317 extreme misalignment. Figure 6 graphically shows the difference in alignment between the
318 template and drill press installed in the same tree as based on the saturation method. In this

319 example, the installation via T5 was deemed successful at 5 mm, with $V_{h,HRM}$ not exceed ± 5 cm
320 hr^{-1} , though not at 15 mm, as the misalignment of the probes had increased with depth.

321

322 **Discussion**

323 As indicated in the introduction, the minimization of misalignment in the installation of
324 sap flux probes has been identified as a major challenge in ensuring accuracy of measurements,
325 though one that can potentially be rectified with proper techniques. To gain some insight into the
326 frequency to which researchers typically employ techniques to avoid misalignment errors, we
327 reviewed a subset of papers published since 2000 that involved HP sap flow measurements.
328 While the use of drilling templates has been repeatedly recommended in meta-analyses of
329 potential sources of error in sap flow studies (Flo et al., 2019; Forster, 2017; Vandegehuchte &
330 Steppe, 2013), their use has not been ubiquitous or consistently documented. Using the search
331 terms “heat pulse”, “sap flow”, “transpiration”, and “water use”, as well as these review papers,
332 36 published articles using a heat pulse method since 2000 were identified. Of these, only 17
333 mentioned the use of a drilling guide (Ballester et al., 2011, 2013; Bleby et al., 2004; Burgess et
334 al., 2001; Clulow et al., 2013; Deng et al., 2021; Doronila & Forster, 2015; Dragoni et al., 2009;
335 Fernández et al., 2006; Forster, 2020; Fuchs et al., 2017; Intrigliolo et al., 2009; Madurapperuma
336 et al., 2009; McJannet & Fitch, 2004; Pearsall et al., 2014; Pfautsch et al., 2011; Wullschleger &
337 King, 2000), only five described the drilling guide in any detail (Bleby et al., 2004; Burgess et
338 al., 2001; Deng et al., 2021; Madurapperuma et al., 2009; McJannet & Fitch, 2004), and just one
339 provided information on the depth of the guide (McJannet & Fitch, 2004). Just over half of the
340 published articles in this review did not use, or did not mention the use of, a drill guide (Alarcon
341 et al., 2005; Ferrara & Flore, 2003; Forster, 2012; Gutiérrez-Soto, 2012; Hernandez-Santana et

342 al., 2015; Looker et al., 2016; Molina et al., 2016; Perez-Priego et al., 2017; Prendergast et al.,
343 2007; Raulier et al., 2002; Skelton et al., 2013; Tfwala et al., 2018; Van de Wal et al., 2015; Xu
344 et al., 2011; Yunusa et al., 2000; M. Zeppel et al., 2010; M. J. B. Zeppel et al., 2011; Zhao et al.,
345 2018). Thus, despite the recognition of probe alignment as vital to accurate sap flow
346 measurements, there still remains a lack of standardization in techniques to minimize
347 misalignment.

348 Analyses in this paper strongly suggest that not all drill guide designs are equivalent and
349 that certain designs should become the standard while others should be discontinued. In
350 particular, there was a substantial difference between the 5 mm drilling template and the 10 mm
351 drilling template in the controlled wood experiment. Intuitively, the successful drill rate declined
352 with depth; no holes drilled via T5 were within ± 0.5 mm of the ideal position at 7.5 cm. The use
353 of a drilling template less than 10 mm in depth would consistently lead to probe misalignment
354 greater than 0.5 mm and error in raw heat pulse velocity measurements that would necessitate a
355 redrill under the saturation, inverse mathematical solution, or over-length methods. When a
356 drilling template is used in HP experiments, it should be of at least 10 mm depth and tested
357 before deployment. Additional methods, such as the overlength and inverse mathematical
358 methods should be used to determine more exact probe spacings, and it can be noted that these
359 two methods found relatively similar results when applied at the same installation.

360 Furthermore, while all drill guide types alleviated lateral and vertical misalignment, the
361 drill press outperformed both templates in minimizing angular misalignment. Based on our
362 review of the literature, this is the first instance of a suggestion for a technique for minimizing
363 angular misalignment, aside from post-hoc corrections. Besides improving accuracy of the
364 measurement of sap flow, use of the drill press can also reduce costs and the time required to

365 start collecting data. Without the drill rig, we would normally need to wait for periods with
366 nighttime precipitation events to assess via Eqn. 3 and the saturation method whether probes
367 were suitably aligned. When they were not properly aligned, the probes would need to be
368 redrilled, requiring additional time in the field, increasing the potential for damaging sensors, and
369 decreasing the sampling period available during the growing season.

370 The portable drill press detailed in this study provided a solution to probe misalignment
371 and would allow for a focus on alternative sources of error, including nocturnal xylem flow (M.
372 Zeppel et al., 2010), radial and circumferential variability (Berdanier et al., 2016), and seasonal
373 variation in thermal diffusivity (Vandegehuchte & Steppe, 2012), when using the HP family of
374 sap flow methods. Aside from the improved performance compared to more traditional drilling
375 guides, this press offers the ability to switch between heat pulse methods by adjusting the
376 spacing of the probes without the need for multiple templates, though results were further
377 improved when the optional template was attached to the drill press. Use of the press without the
378 attachable template would provide researchers with a reliable flexibility to select the heat pulse
379 method best suited to their experiment. Moving forward, we would suggest sap flow researchers
380 use a drill press of similar design to the one detailed in this paper.

381

382 **Data and Materials Availability**

383 The data and materials used to test and design the portable drill press will be made available in a
384 free to access public data repository.

385

386 **Conflict of Interest**

387 None declared.

388

389 **Funding**

390 USDA McIntire-Stennis Program and NSF Hydrological Sciences

391

392 **Acknowledgements**

393 No acknowledgements

394

395 **Authors' Contributions**

396 JB and SS jointly designed the portable drill press. JB tested the device, with guidance from SS.

397 JB prepared the manuscript, with guidance and edits from SS.

398

399

400

401

402

403

404

405

406 **Literature Cited**

- 407 Alarcon, J. J., Ortuno, M. F., Nicolas, E., Torres, R., & Torrecillas, A. (2005). Compensation
408 heat-pulse measurements of sap flow for estimating transpiration in young lemon trees.
409 *Biologia Plantarum*, 49(4), 527–532. <https://doi.org/10.1007/s10535-005-0046-1>
- 410 Ballester, C., Castel, J., Sanz, F., Yeves, A., Intrigliolo, D. S., & Castel, J. R. (2011). Can sap
411 flow probes be used for determining transpiration of citrus trees under different irrigation
412 regimes? *Acta Horticulturae*, 922, 221–228.
413 <https://doi.org/10.17660/ActaHortic.2011.922.29>
- 414 Ballester, C., Castel, J., Testi, L., Intrigliolo, D. S., & Castel, J. R. (2013). Can heat-pulse sap
415 flow measurements be used as continuous water stress indicators of citrus trees?
416 *Irrigation Science*, 31(5), 1053–1063. <https://doi.org/10.1007/s00271-012-0386-5>
- 417 Berdanier, A. B., Miniati, C. F., & Clark, J. S. (2016). Predictive models for radial sap flux
418 variation in coniferous, diffuse-porous and ring-porous temperate trees. *Tree Physiology*,
419 36(8), 932–941. <https://doi.org/10.1093/treephys/tpw027>
- 420 Bleby, T. M., Burgess, S. S. O., & Adams, M. A. (2004). A validation, comparison and error
421 analysis of two heat-pulse methods for measuring sap flow in *Eucalyptus marginata*
422 saplings. *Functional Plant Biology*, 31(6), 645. <https://doi.org/10.1071/FP04013>
- 423 Burgess, S. S. O., Adams, M. A., Turner, N. C., Beverly, C. R., Ong, C. K., Khan, A. A. H., &
424 Bleby, T. M. (2001). An improved heat pulse method to measure low and reverse rates of
425 sap flow in woody plants. *Tree Physiology*, 21(9), 589–598.
426 <https://doi.org/10.1093/treephys/21.9.589>
- 427 Bush, S. E., Hultine, K. R., Sperry, J. S., & Ehleringer, J. R. (2010). Calibration of thermal
428 dissipation sap flow probes for ring- and diffuse-porous trees. *Tree Physiology*, 30(12),
429 1545–1554. <https://doi.org/10.1093/treephys/tpq096>
- 430 Clulow, A. D., Everson, C. S., Price, J. S., Jewitt, G. P. W., & Scott-Shaw, B. C. (2013). Water-
431 use dynamics of a peat swamp forest and a dune forest in Maputaland, South Africa.
432 *Hydrology and Earth System Sciences*, 17(5), 2053–2067. [https://doi.org/10.5194/hess-](https://doi.org/10.5194/hess-17-2053-2013)
433 [17-2053-2013](https://doi.org/10.5194/hess-17-2053-2013)
- 434 Cohen, Y., Fuchs, M., & Green, G. C. (1981). Improvement of the heat pulse method for
435 determining sap flow in trees. *Plant, Cell & Environment*, 4(5), 391–397.
436 <https://doi.org/10.1111/j.1365-3040.1981.tb02117.x>
- 437 Deng, Z., Vice, H. K., Gilbert, M. E., Adams, M. A., & Buckley, T. N. (2021). A double-ratio
438 method to measure fast, slow and reverse sap flows. *Tree Physiology*, 41(12), 2438–
439 2453. <https://doi.org/10.1093/treephys/tpab081>
- 440 Do, F., & Rocheteau, A. (2002). Influence of natural temperature gradients on measurements of
441 xylem sap flow with thermal dissipation probes. 1. Field observations and possible
442 remedies. *Tree Physiology*, 22(9), 641–648. <https://doi.org/10.1093/treephys/22.9.641>
- 443 Doronila, A. I., & Forster, M. A. (2015). Performance Measurement Via Sap Flow Monitoring of
444 Three *Eucalyptus* Species for Mine Site and Dryland Salinity Phytoremediation.

- 445 *International Journal of Phytoremediation*, 17(2), 101–108.
446 <https://doi.org/10.1080/15226514.2013.850466>
- 447 Dragoni, D., Caylor, K. K., & Schmid, H. P. (2009). Decoupling structural and environmental
448 determinants of sap velocity: Part II. Observational application. *Agricultural and Forest*
449 *Meteorology*, 149(3), 570–581. <https://doi.org/10.1016/j.agrformet.2008.10.010>
- 450 Dye, P. J., Olbrich, B. W., & Poulter, A. G. (1991). The Influence of Growth Rings in *Pinus*
451 *patula* on Heat Pulse Velocity and Sap Flow Measurement. *Journal of Experimental*
452 *Botany*, 42(240), 867–870.
- 453 Fernández, J. E., Durán, P. J., Palomo, M. J., Diaz-Espejo, A., Chamorro, V., & Girón, I. F.
454 (2006). Calibration of sap flow estimated by the compensation heat pulse method in
455 olive, plum and orange trees: Relationships with xylem anatomy. *Tree Physiology*, 26(6),
456 719–728. <https://doi.org/10.1093/treephys/26.6.719>
- 457 Ferrara, G., & Flore, J. A. (2003). Comparison Between Different Methods for Measuring
458 Transpiration in Potted Apple Trees. *Biologia Plantarum*, 46(1), 41–47.
459 <https://doi.org/10.1023/A:1022301931508>
- 460 Flo, V., Martínez-Vilalta, J., Steppe, K., Schuldt, B., & Poyatos, R. (2019). A synthesis of bias
461 and uncertainty in sap flow methods. *Agricultural and Forest Meteorology*, 271, 362–
462 374. <https://doi.org/10.1016/j.agrformet.2019.03.012>
- 463 Ford, C. R., McGuire, M. A., Mitchell, R. J., & Teskey, R. O. (2004). Assessing variation in the
464 radial profile of sap flux density in *Pinus* species and its effect on daily water use. *Tree*
465 *Physiology*, 24(3), 241–249. <https://doi.org/10.1093/treephys/24.3.241>
- 466 Forster, M. A. (2012). Quantifying water use in a plant–fungal interaction. *Fungal Ecology*, 5(6),
467 702–709. <https://doi.org/10.1016/j.funeco.2012.06.005>
- 468 Forster, M. A. (2017). How Reliable Are Heat Pulse Velocity Methods for Estimating Tree
469 Transpiration? *Forests*, 8(9), Article 9. <https://doi.org/10.3390/f8090350>
- 470 Forster, M. A. (2019). The Dual Method Approach (DMA) Resolves Measurement Range
471 Limitations of Heat Pulse Velocity Sap Flow Sensors. *Forests*, 10(1), Article 1.
472 <https://doi.org/10.3390/f10010046>
- 473 Forster, M. A. (2020). The importance of conduction versus convection in heat pulse sap flow
474 methods. *Tree Physiology*, 40(5), 683–694. <https://doi.org/10.1093/treephys/tpaa009>
- 475 Fuchs, S., Leuschner, C., Link, R., Coners, H., & Schuldt, B. (2017). Calibration and comparison
476 of thermal dissipation, heat ratio and heat field deformation sap flow probes for diffuse-
477 porous trees. *Agricultural and Forest Meteorology*, 244–245, 151–161.
478 <https://doi.org/10.1016/j.agrformet.2017.04.003>
- 479 Granier, A. (1985). A new method of sap flow measurement in tree stems. *Annals of Forest*
480 *Science*, 45(2), 193–200.
- 481 Gutiérrez-Soto, M. V. (2012). HRM - Heat Ratio Method to Measure Sap Flow in Papaya & Oil
482 Palm. *Environmental Monitoring*, 6.

- 483 Hatton, T. J., Moore, S. J., & Reece, P. H. (1995). Estimating stand transpiration in a Eucalyptus
 484 populnea woodland with the heat pulse method: Measurement errors and sampling
 485 strategies. *Tree Physiology*, *15*(4), 219–227. <https://doi.org/10.1093/treephys/15.4.219>
- 486 Hernandez-Santana, V., Hernandez-Hernandez, A., Vadeboncoeur, M. A., & Asbjornsen, H.
 487 (2015). Scaling from single-point sap velocity measurements to stand transpiration in a
 488 multispecies deciduous forest: Uncertainty sources, stand structure effect, and future
 489 scenarios. *Canadian Journal of Forest Research*, *45*(11), 1489–1497.
 490 <https://doi.org/10.1139/cjfr-2015-0009>
- 491 Hogg, E. H., & Hurdle, P. A. (1997). Sap flow in trembling aspen: Implications for stomatal
 492 responses to vapor pressure deficit. *Tree Physiology*, *17*(8–9), 501–509.
 493 <https://doi.org/10.1093/treephys/17.8-9.501>
- 494 *Implexx Manuals and Guides | Implexx Sense*. (2019, October 27).
 495 <https://www.implexx.io/manuals-and-guides/>
- 496 Intrigliolo, D. S., Lakso, A. N., & Piccioni, R. M. (2009). Using the heat pulse “Tmax”
 497 procedure to estimate grapevine water use in a humid climate. *Acta Horticulturae*,
 498 *No.846*, 177–184.
- 499 Jasechko, S., Sharp, Z. D., Gibson, J. J., Birks, S. J., Yi, Y., & Fawcett, P. J. (2013). Terrestrial
 500 water fluxes dominated by transpiration. *Nature*, *496*(7445), Article 7445.
 501 <https://doi.org/10.1038/nature11983>
- 502 Kluitenberg, G. J., & Ham, J. M. (2004). Improved theory for calculating sap flow with the heat
 503 pulse method. *Agricultural and Forest Meteorology*, *126*(1), 169–173.
 504 <https://doi.org/10.1016/j.agrformet.2004.05.008>
- 505 Kluitenberg, G. J., Ochsner, T. E., & Horton, R. (2007). Improved Analysis of Heat Pulse
 506 Signals for Soil Water Flux Determination. *Soil Science Society of America Journal*,
 507 *71*(1), 53–55. <https://doi.org/10.2136/sssaj2006.0073N>
- 508 Liu, G., Wen, M., Chang, X., Ren, T., & Horton, R. (2013). A Self-Calibrated Dual Probe Heat
 509 Pulse Sensor for In Situ Calibrating the Probe Spacing. *Soil Science Society of America*
 510 *Journal*, *77*(2), 417–421. <https://doi.org/10.2136/sssaj2012.0434n>
- 511 Looker, N., Martin, J., Jencso, K., & Hu, J. (2016). Contribution of sapwood traits to uncertainty
 512 in conifer sap flow as estimated with the heat-ratio method. *Agricultural and Forest*
 513 *Meteorology*, *223*, 60–71. <https://doi.org/10.1016/j.agrformet.2016.03.014>
- 514 Madurapperuma, W. S., Bleby, T. M., & Burgess, S. S. O. (2009). Evaluation of sap flow
 515 methods to determine water use by cultivated palms. *Environmental and Experimental*
 516 *Botany*, *66*(3), 372–380. <https://doi.org/10.1016/j.envexpbot.2009.04.002>
- 517 McJannet, D., & Fitch, P. (2004). A flexible and easily constructed heat pulse system for
 518 monitoring sapflow in trees. *CSIRO Land and Water*, *29*.
- 519 Molina, A. J., Aranda, X., Carta, G., Llorens, P., Romero, R., Savé, R., & Biel, C. (2016). Effect
 520 of irrigation on sap flux density variability and water use estimate in cherry (*Prunus*
 521 *avium*) for timber production: Azimuthal profile, radial profile and sapwood estimation.
 522 *Agricultural Water Management*, *164*, 118–126.
 523 <https://doi.org/10.1016/j.agwat.2015.08.019>

- 524 Pearsall, K. R., Williams, L. E., Castorani, S., Bleby, T. M., McElrone, A. J., Pearsall, K. R.,
525 Williams, L. E., Castorani, S., Bleby, T. M., & McElrone, A. J. (2014). Evaluating the
526 potential of a novel dual heat-pulse sensor to measure volumetric water use in grapevines
527 under a range of flow conditions. *Functional Plant Biology*, *41*(8), 874–883.
528 <https://doi.org/10.1071/FP13156>
- 529 Perez-Priego, O., El-Madany, T. S., Migliavacca, M., Kowalski, A. S., Jung, M., Carrara, A.,
530 Kolle, O., Martín, M. P., Pacheco-Labrador, J., Moreno, G., & Reichstein, M. (2017).
531 Evaluation of eddy covariance latent heat fluxes with independent lysimeter and sapflow
532 estimates in a Mediterranean savannah ecosystem. *Agricultural and Forest Meteorology*,
533 *236*, 87–99. <https://doi.org/10.1016/j.agrformet.2017.01.009>
- 534 Pfautsch, S., Keitel, C., Turnbull, T. L., Braimbridge, M. J., Wright, T. E., Simpson, R. R.,
535 O'Brien, J. A., & Adams, M. A. (2011). Diurnal patterns of water use in *Eucalyptus*
536 *victrix* indicate pronounced desiccation–rehydration cycles despite unlimited water
537 supply. *Tree Physiology*, *31*(10), 1041–1051. <https://doi.org/10.1093/treephys/tpr082>
- 538 Prendergast, P., Astill, M., Green, S., Mills, T., & Clothier, B. (2007). Water Use by a Kiwifruit
539 Vine: Calibration, Measurements and a Model. *Acta Horticulturae*.
540 <https://doi.org/10.17660/ActaHortic.2007.753.70>
- 541 Raulier, F., Bernier, P. Y., Ung, C.-H., & Boutin, R. (2002). Structural differences and functional
542 similarities between two sugar maple (*Acer saccharum*) stands. *Tree Physiology*, *22*(15–
543 16), 1147–1156. <https://doi.org/10.1093/treephys/22.15-16.1147>
- 544 Ren, R., Liu, G., Wen, M., Horton, R., Li, B., & Si, B. (2017). The effects of probe misalignment
545 on sap flux density measurements and in situ probe spacing correction methods.
546 *Agricultural and Forest Meteorology*, *232*, 176–185.
547 <https://doi.org/10.1016/j.agrformet.2016.08.009>
- 548 Roddy, A. B., & Dawson, T. E. (2013). Novel patterns of hysteresis in the response of leaf-level
549 sap flow to vapor pressure deficit. *Acta Horticulturae*, *991*, 261–267.
550 <https://doi.org/10.17660/ActaHortic.2013.991.32>
- 551 Skelton, R. P., West, A. G., Dawson, T. E., & Leonard, J. M. (2013). External heat-pulse method
552 allows comparative sapflow measurements in diverse functional types in a
553 Mediterranean-type shrubland in South Africa. *Functional Plant Biology*, *40*(10), 1076–
554 1087. <https://doi.org/10.1071/FP12379>
- 555 Steppe, K., De Pauw, D. J. W., Doody, T. M., & Teskey, R. O. (2010). A comparison of sap flux
556 density using thermal dissipation, heat pulse velocity and heat field deformation methods.
557 *Agricultural and Forest Meteorology*, *150*(7), 1046–1056.
558 <https://doi.org/10.1016/j.agrformet.2010.04.004>
- 559 Swanson, R. H., & Whitfield, D. W. A. (1981). A Numerical Analysis of Heat Pulse Velocity
560 Theory and Practice. *Journal of Experimental Botany*, *32*(126), 221–239. JSTOR.
- 561 Tfwala, C. M., van Rensburg, L. D., Bello, Z. A., & Green, S. R. (2018). Calibration of
562 compensation heat pulse velocity technique for measuring transpiration of selected
563 indigenous trees using weighing lysimeters. *Agricultural Water Management*, *200*, 27–
564 33. <https://doi.org/10.1016/j.agwat.2018.01.005>

565 Van de Wal, B. A. E., Guyot, A., Lovelock, C. E., Lockington, D. A., & Steppe, K. (2015).
566 Influence of temporospatial variation in sap flux density on estimates of whole-tree water
567 use in *Avicennia marina*. *Trees*, *29*(1), 215–222. <https://doi.org/10.1007/s00468-014->
568 1105-z

569 Vandegehuchte, M. W., & Steppe, K. (2012). Improving sap flux density measurements by
570 correctly determining thermal diffusivity, differentiating between bound and unbound
571 water. *Tree Physiology*, *32*(7), 930–942. <https://doi.org/10.1093/treephys/tps034>

572 Vandegehuchte, M. W., & Steppe, K. (2013). Sap-flux density measurement methods: Working
573 principles and applicability. *Functional Plant Biology*, *40*(3), 213.
574 <https://doi.org/10.1071/FP12233>

575 Wullschleger, S. D., & King, A. W. (2000). Radial variation in sap velocity as a function of stem
576 diameter and sapwood thickness in yellow-poplar trees. *Tree Physiology*, *20*(8), 511–518.
577 <https://doi.org/10.1093/treephys/20.8.511>

578 Xu, X., Tong, L., Li, F., Kang, S., & Qu, Y. (2011). Sap flow of irrigated *Populus alba* var.
579 *Pyramidalis* and its relationship with environmental factors and leaf area index in an arid
580 region of Northwest China. *Journal of Forest Research*, *16*(2), 144–152.
581 <https://doi.org/10.1007/s10310-010-0220-y>

582 Yunusa, I. A. M., Walker, R. R., Loveys, B. R., & Blackmore, D. H. (2000). Determination of
583 transpiration in irrigated grapevines: Comparison of the heat-pulse technique with
584 gravimetric and micrometeorological methods. *Irrigation Science*, *20*(1), 1–8.
585 <https://doi.org/10.1007/PL00006714>

586 Zeppel, M. J. B., Lewis, J. D., Medlyn, B., Barton, C. V. M., Duursma, R. A., Eamus, D.,
587 Adams, M. A., Phillips, N., Ellsworth, D. S., Forster, M. A., & Tissue, D. T. (2011).
588 Interactive effects of elevated CO₂ and drought on nocturnal water fluxes in *Eucalyptus*
589 *saligna*. *Tree Physiology*, *31*(9), 932–944. <https://doi.org/10.1093/treephys/tpr024>

590 Zeppel, M., Tissue, D., Taylor, D., Macinnis-Ng, C., & Eamus, D. (2010). Rates of nocturnal
591 transpiration in two evergreen temperate woodland species with differing water-use
592 strategies. *Tree Physiology*, *30*(8), 988–1000. <https://doi.org/10.1093/treephys/tpq053>

593 Zhao, X., Guo, P., Zhang, Z., Wang, X., Peng, H., & Wang, M. (2018). Wood Density and Fiber
594 Dimensions of Root, Stem, and Branch Wood of *Populus ussuriensis* Kom. *Trees*.
595 *BioResources*, *13*(3), Article 3.

596

597

598

599

600

601

602

603

604

605

606

607 **List of Tables and Figures**

608 **1. Figure 1**

609 **2. Figure 2**

610 **3. Figure 3**

611 **4. Figure 4**

612 **5. Table 1**

613 **6. Table 2**

614 **7. Figure 5**

615 **8. Figure 6**

616

617

618

619

620

621

622

623

624

625

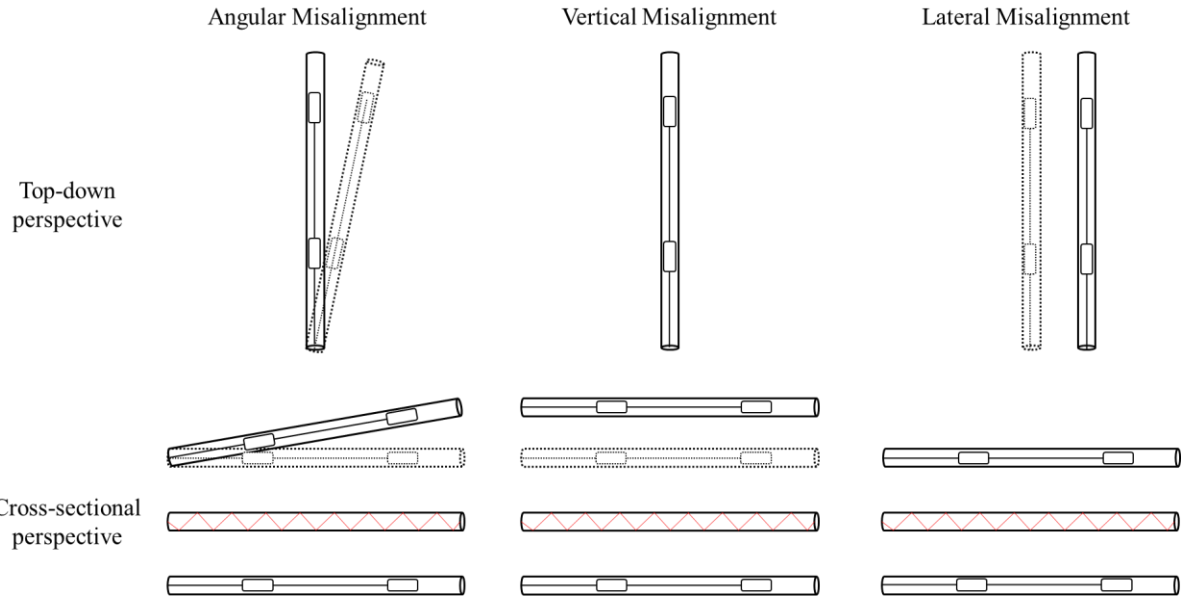
626

627

628

629

630



631

632 **Figure 1:** Three types of probe misalignment portrayed from the top-down and cross-sectional
 633 perspectives. Angular probe misalignment can occur in the lateral and vertical direction.
 634

635

636

637

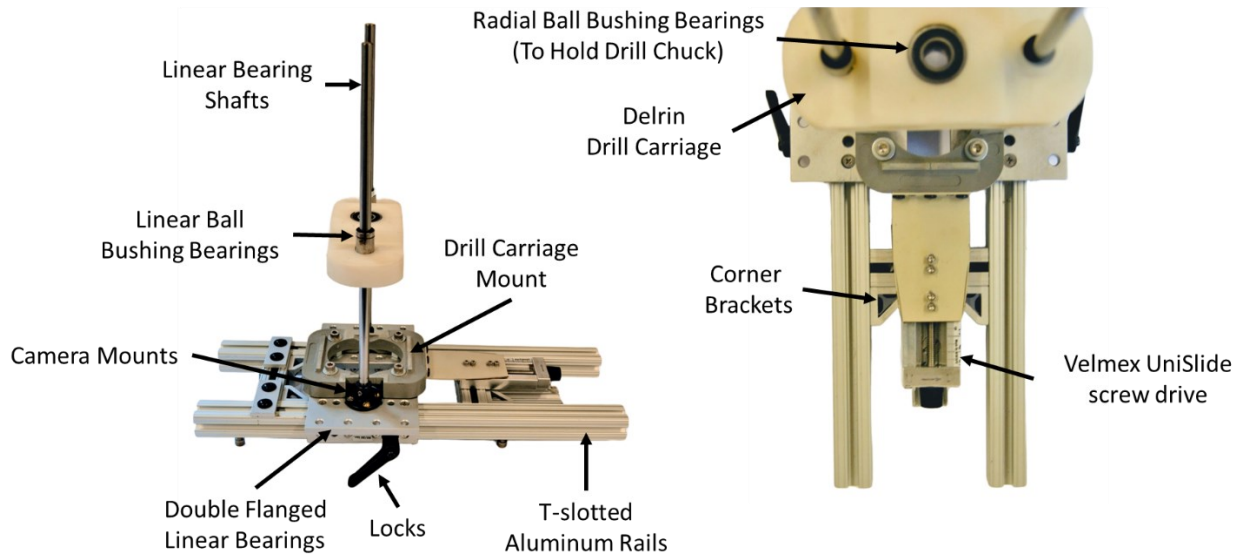
638

639

640

641

642



643

644

645 **Figure 2:** Annotated images of the portable drill press detailing the parts used in construction.

646

647

648

649

650

651

652

653

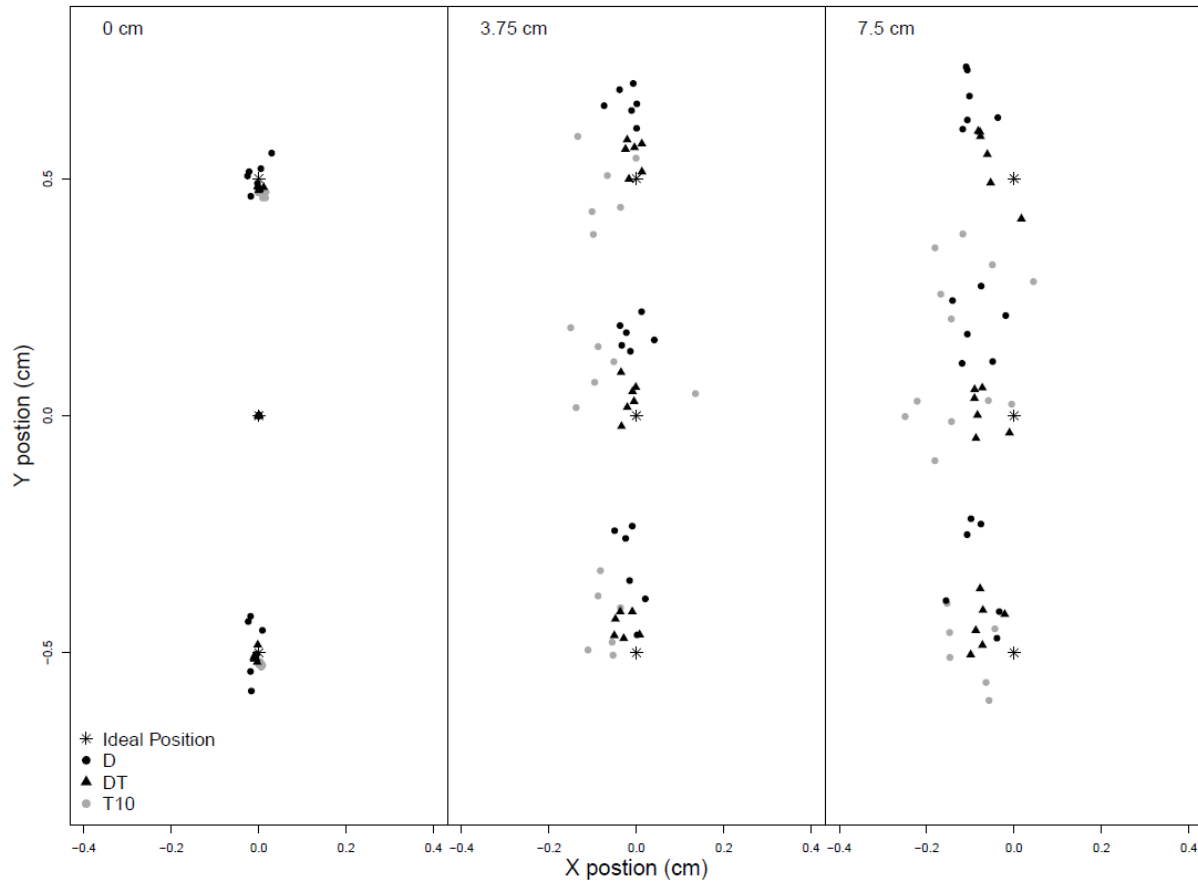
654



655

656 **Figure 3:** Image of the drill press mounted on a mature tree in the field using a ratchet strap.

657



658

659 **Figure 4:** Position of each exit wound in wood block relative to the ideal position of -5, 0, 5 mm
 660 for the upstream, heater and downstream probe, respectively, at 0 (i.e., entry; left), 3.75 cm
 661 (middle) and 7.5 cm (right). Generally, the drill press (black) was more accurate along the lateral
 662 direction than the 10 mm deep drilling template (light grey), and both were more accurate than
 663 the 5 mm deep drilling template.

664

665

666

667

668

669

670

671

672

673

674 **Table 1:** Mean and standard deviation (in parentheses) of absolute misalignment in the vertical
 675 and lateral directions at entry for each drill guide.

676

| Drill Guide Type | Lateral Misalignment (mm) | Vertical Misalignment (mm) |
|-------------------------|----------------------------------|-----------------------------------|
| DT | 0.03 (0.04) | 0.11 (0.08) |
| D | 0.10 (0.10) | 0.25 (0.27) |
| T10 | 0.05 (0.05) | 0.19 (0.15) |
| T5 | 0.09 (0.16) | 0.29 (0.30) |

677

678

679

680

681

682

683

684

685

686

687

688

689

690

691

692

693

694

695

696

697

698

699

700

701

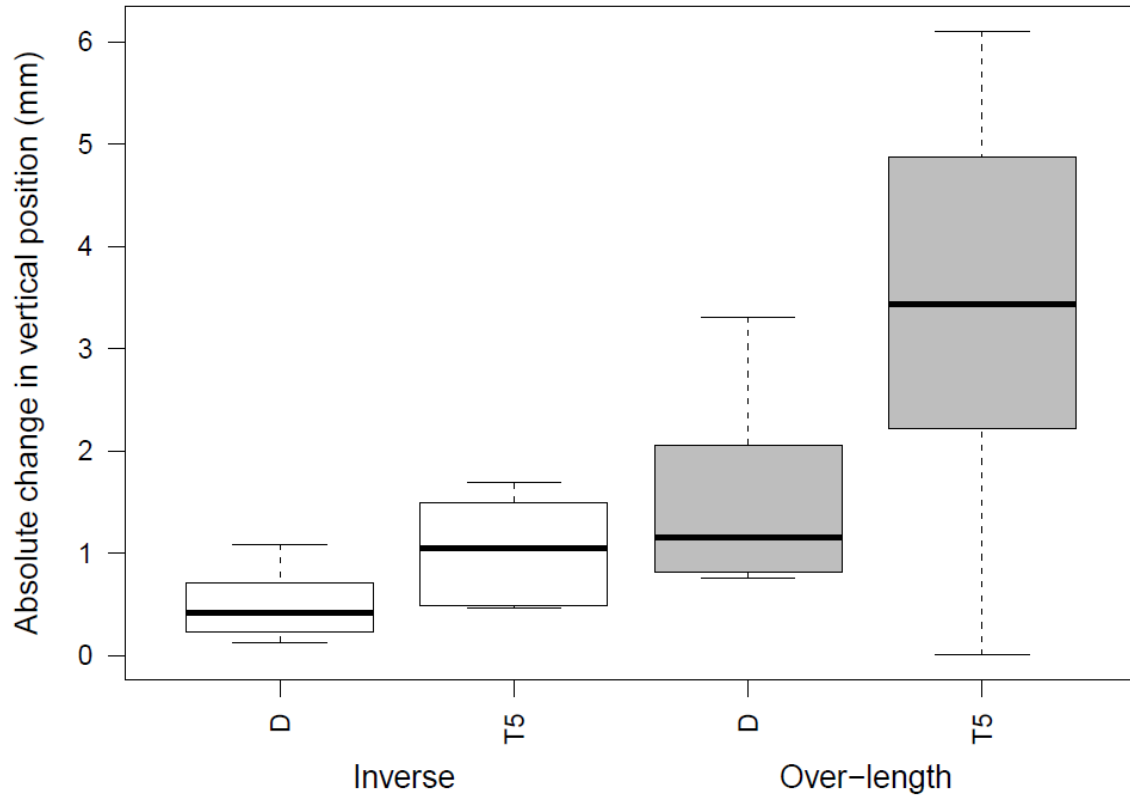
702

703 **Table 2:** Mean, standard deviation (in parenthesis), and mean absolute error of the vertical and
704 lateral angular misalignment.

705

| Drill Guide Type | Mean vertical angle (°) | Vertical MAE (°) | Mean lateral angle (°) | Lateral MAE (°) |
|------------------|-------------------------|------------------|------------------------|-----------------|
| DT | 0.37 (0.46) | 0.49 | -0.49 (0.24) | 0.51 |
| D | 1.07 (0.48) | 1.07 | 0.21 (0.40) | 0.35 |
| T10 | -0.36 (0.82) | 0.68 | -0.93 (0.59) | 0.96 |
| T5 | 5.44 (1.88) | 5.43 | 3.47 (3.02) | 3.9 |

706
707
708
709
710
711
712
713
714
715
716
717
718
719
720
721
722
723
724
725
726
727
728
729
730



731

732 **Figure 5:** Absolute change in vertical position of the up- and downstream probes across all
 733 instrumented trees between the drill press (D) and the drilling template (T5) determined via the
 734 inverse mathematical (white) and over-length (grey) methods. The inverse mathematical method
 735 assesses the change in position from the shallowest thermistor (5 mm) to the deepest (35 mm)
 736 while the over-length method accounts for change in position across the entire length of the probe
 737 (50 mm).

738

739

740

741

742

743

744

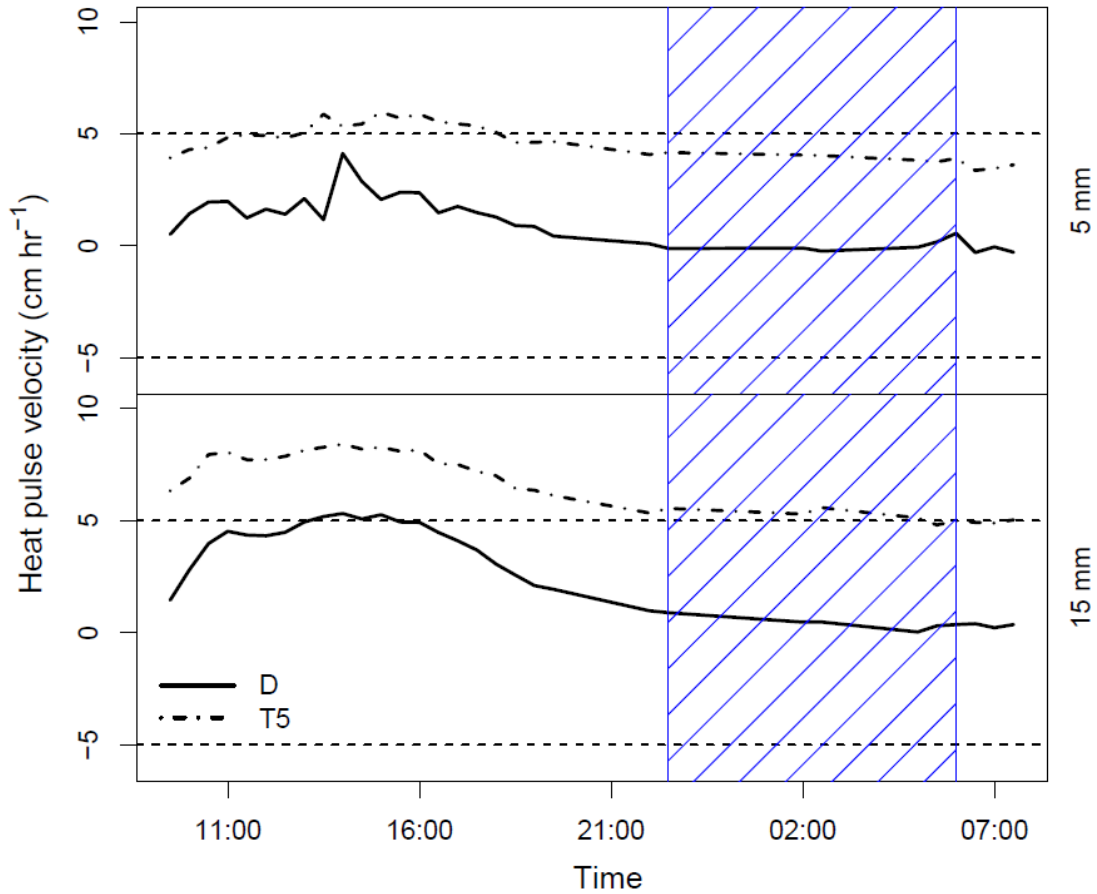
745

746

747

748

749



750

751 **Figure 6:** Example of heat pulse velocity measurements ($V_{h,HRM}$) via the drill press (D; solid
 752 line) and the 5 mm drilling template (T5; dashed and dotted line) during a nighttime precipitation
 753 event (blue hashing), for two radial depths in Hem-3. Each Installations where $V_{h,HRM}$ fell outside
 754 the -5 to 5 cm hr^{-1} threshold (dashed line) during the nighttime precipitation event (bottom) were
 755 identified as overly misaligned and requiring of a redrill. Installations that fell within this
 756 threshold (top) were identified as aligned or suitable for post-hoc corrections, such as the
 757 saturation method.

758